Tunneling in multilayer fullerene/Al_2O_3 and fullerene/Ge systems

S. Nolen and S. T. Ruggiero
University of Notre Dame, Notre Dame, Indiana 46556
(Received 27 January 1998; revised manuscript received 19 June 1998)

We discuss results on tunneling in barriers consisting of both pure fullerene films and layered composites of fullerenes and dielectric materials. This work focuses on C_{60} films, which ranged from 50 to 600 Å in thickness and were layered with both Al_2O_3 and Ge films 10 to 40 Å in thickness. These studies reveal that for the deposition conditions used here, incomplete C_{60} coverage occurred for film thicknesses less than ~400 Å. For composites of C_{60} with Al_2O_3 or Ge, we observed isolated clusters of C_{60} molecules and Coulomb blockade behavior consistent with the size scale of the clusters. Interesting dynamical effects were also observed in conductance characteristics that were both dramatic and in some cases entirely reproducible.
[S0163-1829(98)02440-0]

I. INTRODUCTION

Fullerenes have certainly captured the imagination of the scientific community because of their truly unique characteristics. New electronic and materials properties, as well as the exciting potential for a variety of applications, continue to fuel broad investigations in this new field of research. Good reviews[1,2] and an abstract list[3] are available on the subject.

In this paper we discuss electron tunneling in pure fullerene thin films and in layered composites of fullerene and dielectric films. In the present work we focus on the basic tunneling properties of these systems which have been found to reveal much about the nature of the fullerenes. The work stems from the process of optimizing the characteristics of these C_{60} and C_{70} systems for inelastic electron tunneling spectroscopy (IETS) work, which will be the topic of a future publication.

The general approach to junction fabrication follows traditional lines in terms of the creation of metal/barrier/metal ($M/B/M$) type systems where each element is a thin-film layer. In this work, the barrier layer is either pure C_{60} or a layered composite of C_{60} with either Al_2O_3 or Ge. The use of composite barriers arose from the as-deposited nature of the C_{60} films, which scanning transmission electron microscopy (STEM) and atomic force microscopy (AFM) show to be composed of islandlike clusters with largest size scales on the order of ~100 nm. For pure C_{60}, it was found that complete coverage did not occur until average film thickness reached ~400 Å. A ubiquitous Coulomb blockade was also present, consistent with the presence of isolated clusters. These multilayer tunnel systems also tended to exhibit interesting dynamical effects clearly manifest in both the tunneling resistance and the magnitude of the Coulomb blockade, which in some cases were entirely repeatable.

These and other results have stemmed from the success of creating viable tunnel barriers of fullerene molecules by layering the material with an artificial dielectric barrier material. Surprisingly, the best results have come with the use of germanium. Even though each material—Ge and the fullerenes—individually tends to form films full of pinholes, we find that layered together they form a useful medium for tunneling studies.

Artificial barriers were originally considered for this work because of the successful historical precedent of their use. Noteworthy is their application to superconducting materials which have inadequate native oxides. A good example is Nb, whose native tunneling oxide can be successfully replaced by depositing and then oxidizing a thin surface layer of a metal that forms a good oxide. Such materials include Al,[4–6] Ta,[7] Mg, Y, or Er.[8] For a variety of reasons, Al has emerged as the material of choice for this application.

Another approach to forming a barrier has been to directly deposit oxides such as Al_2O_3, MgO, and SiO_2, fluorides such as AlF_3 and ZrF_4, and other systems including Ti-Si and AlN. Semiconductors, of course, are also a logical choice for barriers. Some materials explored include Si, Ge, and Te. Si has emerged as the semiconductor barrier material of choice, especially in hydrated form. Indeed, Si barriers have also proved to be a rich system for fundamental tunneling studies.[9] The topic of artificial barriers has been reviewed at length.[10]

In light of the above, Al_2O_3 and Ge were chosen for this work because of their known barrier characteristics and their compatibility with thermal evaporation, which was also used for fullerene deposition and for the deposition of the base and counterelectrodes. We also note that amorphous carbon has been used as a barrier material,[11,12] suggesting the basic feasibility of using fullerene thin films themselves as barriers. Furthermore, subsequent to the completion of this work, we found that superimposed thin layers of amorphous carbon and amorphous germanium had previously been used to make successful junctions.[12] In those junctions, the individual germanium and carbon layers were always found to be discontinuous at the thicknesses used, but when superimposed, pinholes were filled.

As discussed by Lieber and Chen,[13] C_{60} can be readily evaporated (or sublimed) like other thin-film materials.[14–16] In this work, fullerene films were thermally evaporated from purified powder with rates in the 1–3 Å/s range.

The samples prepared for our studies fell into two basic classes. Those of the form M/fullerene/M and M/fullerene–dielectric/M, i.e., tunnel junctions with pure C_{60} barriers and junctions with composite barriers of fullerene thin films layered with either Al_2O_3 (an oxidized thin film of Al) or Ge.

 © 1998 The American Physical Society

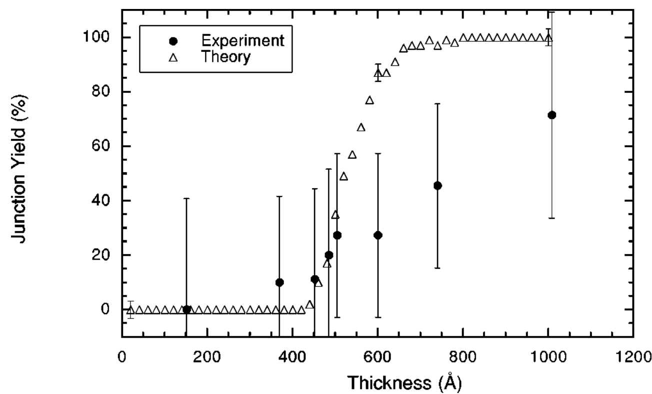

FIG. 1. Junction yield as a function of thickness for metal/C_{60}/metal tunnel junctions Experimental results are represented by closed circles (●). Successful junctions were those that exhibited nonshorted behavior. We also show results for a model of the system (△) that assumes the C_{60} molecules randomly hit the lattice and stick wherever they land. In the model, a successful junction is created when every cell in the lattice contains at least one molecule.

II. RESULTS ON PURE C_{60} LAYERS

Our initial approach was to simply prepare $M/C_{60}/M$ systems. This could, in principle, give an immediate picture of the barrier properties of C_{60} films, including phonon structure. The latter is suggested by tunneling studies of Ge films, which clearly show expected phonon peaks in tunneling conductance.[17] We verified this in M/Ge/M structures with very thick Ge layers and in Ge/C_{60} multilayers where the 11-meV mode (transverse acoustic) was observed and the 34-meV mode (transverse optic) may have been present but was usually obscured by C_{60} molecular vibrations.

The use of pure C_{60} barriers was only marginally successful, however, due to the intrinsic nature of the films. The issue is clearly illustrated by a plot of the success rate of creating viable junctions versus the thickness of the deposited C_{60} (Fig. 1). Viable junctions were arbitrarily defined as those which had measurable resistances—i.e., over about 1 Ω for a junction area of 9.3×10^{-3} cm^2. Very low junction resistances were suspected of being associated with pinholes in the C_{60}, allowing for direct metal to metal contact. However, attempts to create superconducting shorts using Pb as both the base and counterelectrodes were not successful. Some ''successful'' junctions showed the characteristic paraboliclike increase in conductance with increasing bias associated with tunneling while others in this category showed only Ohmic behavior. In any case, by this measure there is clearly a ''turn on'' in the production of successful junctions in the vicinity of 400 Å where it apparently becomes statistically likely for complete film coverage to occur.

We modeled this behavior by treating film growth as the accumulation of randomly deposited C_{60} molecules, with a nearest-neighbor distance of 10 Å. We assumed that the molecules were incident on a set of cells that made up a square, two-dimensional lattice. The molecules were assumed to randomly hit the lattice and stick in whichever cell they landed. Complete coverage of the surface, and thus ''success'' occurred when every cell in the lattice contained at least one molecule. This approach had worked successfully in the description of metal droplets on a surface.[18] Here the model

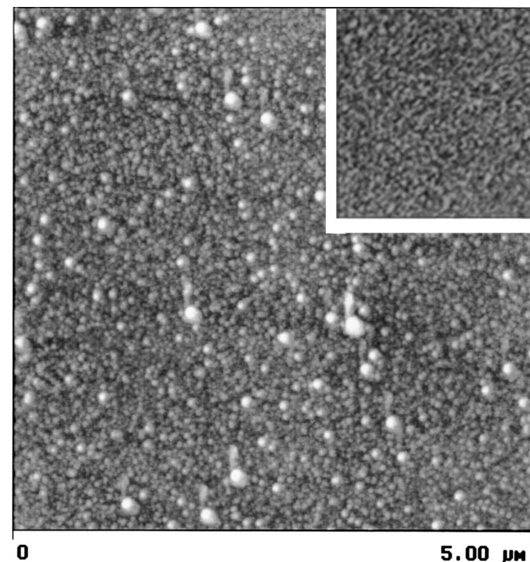

FIG. 2. Tapping mode AFM image of a 101-Å-thick C_{60} film thermally evaporated onto a Cu base electrode. The C_{60} molecules are seen to coalesce to form clusters. The dimensions of the area imaged are 5.0 μm×5.0 μm. Inset is the image of the Cu base electrode at the same magnification. The Cu layer is featureless on this scale and appears not to contribute to the clustering of the C_{60} film.

shows a turn on in the success rate for C_{60} layers in the vicinity of 400 Å and thus a good correlation of theory with observed results. Notwithstanding the success of this approach, film structure was found to be far more complex than this simple model would suggest. This is apparent from surface studies of the films.

AFM studies of the films show that the C_{60} molecules coalesce to form isolated clusters analogous to the way some metal atoms form small islands.[19] Figure 2 is a typical (tapping mode) AFM image of a 101-Å C_{60} film on Cu, prepared in the same manner as that used in $M/C_{60}/M$ tunnel junction formation. The figure clearly shows the presence of C_{60} clusters. The inset in Fig. 2 was an AFM image (at the same magnification) of the Cu base electrode on which the C_{60} film was deposited. On this scale, the film appears to be featureless. AFM images of thicker C_{60} films show an increase in average cluster diameter that scales approximately with film thickness (see Fig. 3).

In any case, because of various technical impracticalities associated with tunneling in films 400 Å or more in thickness and the overall relatively low success rate of making junctions with such thick films—raising the question of junction uniformity—another tact was taken in the exploration of these films. The basic philosophy was to use relatively thin C_{60} films—which are assumed to have pinholes—and fill in the pinholes with a dielectric material. Our various approaches and results follow.

III. COMPOSITE C_{60}/DIELECTRIC SYSTEMS

A. Al_2O_3/C_{60} systems

These junctions (samples 1–7 in Table I) were made by depositing a thin layer of Al (11–12 Å) on top of a thermally evaporated Cu base electrode, without breaking vacuum de-

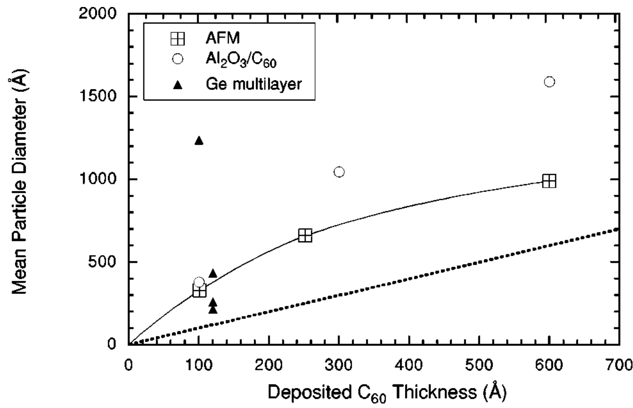

FIG. 3. Mean C_{60} cluster diameter as a function of deposited film thickness. Cluster diameter was determined by the examination of AFM images. Also shown is the effective cluster size based on the magnitude of the Coulomb blockade for individual junctions.

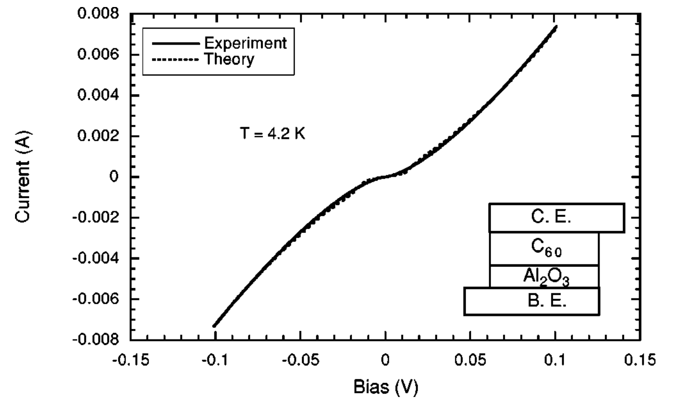

FIG. 4. Tunneling current vs junction bias for a typical BE/Al_2O_3-C_{60}/CE system (sample 1). Here we note the Coulomb blockade near zero bias. The theoretical fit is for the semiclassical double-junction model (Refs. 23 and 24) with $R_1R_2=10\ \Omega$ and $C_1,C_2=6.5\times10^{-18}$ F. A nonlinear background term ($\propto V^3$) is added to the tunneling rate, and a shunt resistance of 67 Ω is added in parallel to the entire junction.

positing a fullerene film (100–600 Å), oxidizing the Al/C_{60} bilayer, and finally depositing a counterelectrode of silver or lead to form a Cu/Al_2O_3/CE sample. The philosophy again was to attempt to fill in pinholes in the C_{60} film with Al_2O_3. We note that this approach has been generally successful with Si barriers on Nb.[20,21] We verified that the Al formed a continuous layer, and thus a good Al_2O_3 barrier, by preparing Cu/Al_2O_3/Pb junctions. The Al_2O_3 in the Cu/Al_2O_3/Pb junctions was formed by the deposition of 12 Å of Al in exactly the same manner as with the other samples studied. These Cu/Al_2O_3/Pb junctions exhibited good tunneling characteristics—low leakage, calculated barrier heights[22] of 1–2 eV, and barrier widths of ~12 Å.

TABLE I. Listed below are the measured and calculated tunnel barrier parameters for composite C_{60}/dielectric systems. Samples are generally comprised as metal/C_{60}–dielectric/metal. The deposited thicknesses are those of the individual Al_2O_3, Ge, or C_{60} layers in the $Al_2O_3/C_{60}$and C_{60}/Ge multilayer barriers. For junctions exhibiting dynamical effects (see Sec. III C), the results are those for the state in which the junction remained the longest.

Sample number	Deposited dielectric thickness (Å)	Deposited fullerene thickness (Å)	RA (Ω cm^2)	Barrier height ϕ (eV)	Barrier width d (Å)
1	15.4[a]	100	0.138	0.384	28.7
2	15.4[a]	100	0.107	1.17	17.2
3	14.1[a]	150	0.070	0.768	20.6
4	14.1[a]	200	0.330	0.705	22.9
5	14.1[a]	252	0.167	0.357	30.4
6	14.1[a]	302	1.350	0.883	22.2
7	14.1[a]	600	0.126	0.580	23.9
8	26.0[b]	100	0.0163	0.609	20.0
9	26.0[b]	100	0.247	0.893	19.6
10	26.0[b]	100	0.115	0.358	28.5
11	20.0[b]	50	0.0558	0.930	17.4
12	20.0[b]	50	0.0425	0.495	22.7
13	35.0[b]	120	0.320	0.251	35.2
14	35.0[b]	120	0.0791	0.317	31.4
15	35.0[b]	120	0.247	0.392	26.6

[a] Al_2O_3.
[b] Ge.

Shown in Fig. 4 is a typical current versus voltage plot for these systems (sample 1). On a gross scale, the first thing to notice is the strong Coulomb blockade near zero bias. Because of the fact that the C_{60} molecules tend to form clusters with a mean diameter on the order of the deposited film thickness (Sec. II), this behavior is not unexpected. Indeed, the presence of a blockade was observed in all Al_2O_3/C_{60} and Ge/C_{60} multilayer samples although was generally clearest in Al_2O_3/C_{60} systems. We took the standard approach in modeling these data, using the semiclassical double-junction model.[23,24] The model is for a M/*B*/*C*/*B*/M structure where M represents metal base and counterelectrodes, and where there are two tunnel barrier layers *B* sandwiched between *C*, which is an ultrasmall capacitance element. One factor in the modeling of our junctions was the ubiquitous presence of some ''leakage'' or nontunneling conductance, which is evident at zero bias. This leakage was in excess of the expected thermally activated conductance at 4.2 K with or without a Coulomb blockade. This was accommodated in the fit by introducing a simple, voltage-independent parallel shunt resistance.[25] For our Al_2O_3/C_{60} samples, this resistance was typically three times the tunneling resistance.

The second issue is the absence of a Coulomb staircase, a series of steps of voltage width e/C, which can follow the Coulomb blockade at zero bias.[26] The absence of a staircase can arise from a number of circumstances. Here, good fits to our data were consistently obtained with the simple assumption that the junctions were symmetric. That is, the product of resistance and capacitance R_1C_1 associated with tunneling onto the central capacitive element was equal to R_2C_2, the parameters associated with tunneling off the central element. These results were also generally consistent with the Giaever-Zeller model,[27] which inherently assumes junction symmetry. Other possibilities that would also tend to eliminate the manifestation of a staircase include a broad distribution of particle sizes.[25] However, for all of our samples, the observed distributions of C_{60} cluster sizes had half-widths σ of ~25–40 % of the average cluster diameter.

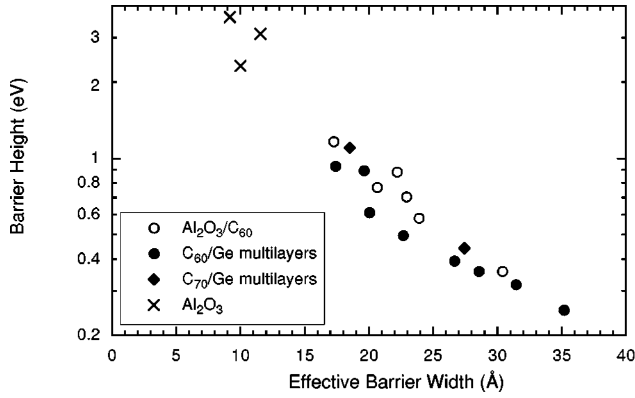

FIG. 5. Effective barrier height vs effective tunnel barrier width as calculated from conductance data taken at 4.2 K. Results for pure Al_2O_3 are included for comparison.

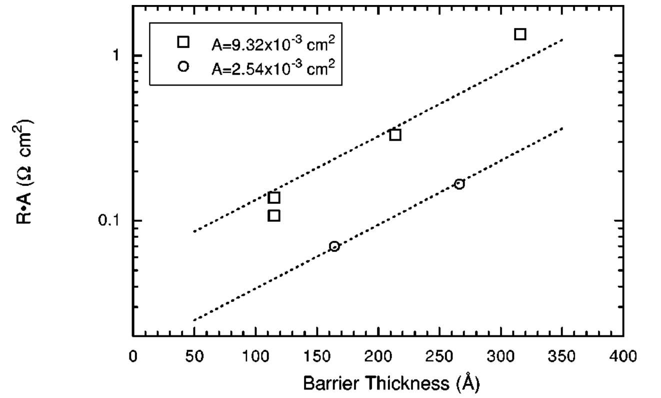

FIG. 6. Resistance times area as a function of deposited thickness for $BE/Al_2O_3-C_{60}/CE$ junctions. The individual trends are associated with somewhat different fabrication techniques.

However, it has been shown that a staircase is not completely washed out even for half-widths of 50%.[25] Thus the observed distribution width of particle size for our samples is not sufficient to describe the absence of staircase behavior. Another possibility for the absence of a staircase is the presence of a series array of junctions.[28,29] However, because of the wide array of C_{60}/dielectric systems examined, it seems unlikely that we could consistently achieve the physical configuration required in this case.

Assuming that the capacitance of the clusters is given simply by $C=2\pi\epsilon_o\epsilon d$, where d is the cluster diameter and ϵ is the dielectric constant for aluminum or germanium as appropriate, we have also extracted the effective cluster size from fits to the tunneling conductance, as presented in Fig. 3. We see that there is a general increase in calculated cluster size, coincident with an observed increase in cluster size with increased deposited C_{60} thickness. However, there also appears to be considerable variability in the physical constitution of junctions with the same nominal C_{60} thickness.

As discussed in the next section, the results of C_{60}/Ge multilayer systems analyzed in this same manner are also noteworthy. In this case, data are available only for relatively thin C_{60} layers, but the majority of these systems can also be described well by the semiclassical double-junction model.

We have also analyzed the basic barrier properties of these systems. The basic approach was to simply account for the Coulomb blockade by a voltage offset and fit to the Simmons result for a simple trapezoidal barrier.[30] The results of this procedure are shown in Fig. 5. (The parallel resistance, discussed above, was not incorporated into these calculations and its presence does not substantially change these results.) The data are consistent with the idea of a systematic depression of the intrinsic barrier height of pure Al_2O_3 as we have previously discussed in connection with Bi particles on Al_2O_3[31] and has been noted in connection with other artificial barrier systems.[7] In general, thicker C_{60} layers produced barriers with progressively lower effective heights and larger widths.

Another perspective on these systems can be gained by a plot of resistance times area, RA, versus thickness (Fig. 6). We expect that

$$RA=3.17\times10^{-11}\left(\frac{t}{\sqrt{\phi}}\right)e^{1.025t\sqrt{\phi}}, \quad (1)$$

(where ϕ is the effective barrier height and t the barrier width), which can be expressed more simply as

$$RA\propto e^{t/\alpha} \quad (2)$$

where α is the characteristic tunneling length.

In Fig. 6 we have plotted RA as a function of the total barrier thickness, which includes both the deposited C_{60} thickness and the estimated thickness for the Al_2O_3 layer. Our results show that $\alpha=86$ Å, which is large compared to the tunneling length for either Al_2O_3 or even typical artificial semiconductor barriers and implies a barrier height of less than 1 meV. Since it is observed (Fig. 5) that individual junctions exhibit relatively large barrier heights, we interpret the RA behavior as simply showing that increasing the C_{60} thickness has only a weak effect on the more dominant underlying Al_2O_3 barrier. We note that similar systematics were observed in the metal fluoride systems.[32]

Interestingly, junctions made with different areas, although exhibiting the same slope, did not fall on the same RA line as expected. However, there is again a precedent for such behavior in other artificial-barrier systems.[33] We note that for our work, the area was changed by edge protection with germanium, and this may have affected the barrier properties through an unanticipated interaction of the C_{60} layers and the germanium.

B. Multilayer Ge/C_{60} systems

In these systems, a fullerene layer is deposited on the thermally evaporated base electrode, followed by a Ge layer. This process is repeated two (samples 8–10 and 13–15) to three (samples 11 and 12) times, and the barrier is topped off with another fullerene layer before the counterelectrode is deposited. For a given junction, individual Ge layers were the same thickness, as were the individual C_{60} layers. The junctions generally had C_{60} to Ge total thickness ratios of 5 to 1. It was found that the total thickness of Ge had to be in excess of about 50 Å or else the junctions would be shorted. Individual Ge layer thicknesses ranged from 20 to 35 Å. Shown in Fig. 7 is a typical current versus voltage plot for these systems (sample 14). The fit is from the aforementioned double-junction model with a shunt resistor added in parallel.

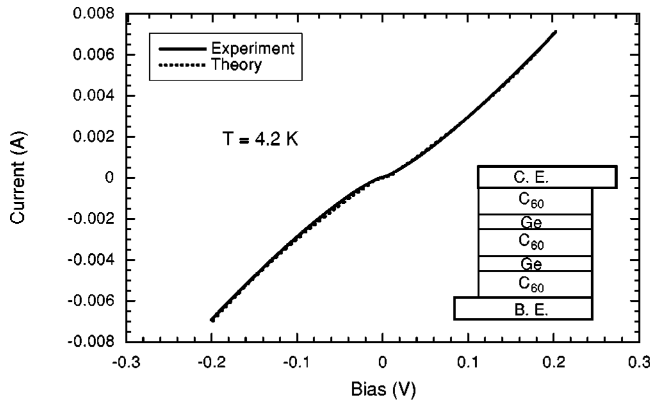

FIG. 7. Tunneling current vs junction bias for a typical BE/C_{60}-Ge multilayer/CE junction (sample 14). The theoretical fit is for the semiclassical double-junction model with $R_1, R_2 = 29\ \Omega$ and $C_1, C_2 = 7.0\times 10^{-18}$ F. A nonlinear background term ($\propto V^3$) is added to the tunneling rate, and a shunt resistance of 77 Ω is added in parallel to the entire junction.

Barrier heights and widths were calculated by fitting the I-V data to the Simmons model as discussed above. Here we found that barrier heights ranged from 0.4 to 0.9 eV for Ge layer thickness less than 30 Å and were much smaller for thicker films. These results are shown in Fig. 5 and include some preliminary results on C_{70}-based systems as well. All systems show a systematic correlation of generally decreasing effective barrier height with increasing effective barrier width.

Remarkable in regard to Ge/C_{60} results was the ability to make a one-to-one correlation between the deposited thickness of individual Ge layers and the effective barrier width, as shown in Fig. 8. The barrier width calculated from the Simmons model and the actual deposited Ge thickness were quite consistent over a relatively wide range of Ge thickness, lending confidence to the procedure used to extract barrier parameters. This was not the case for the Al barriers where calculated barrier thickness was consistently greater than the deposited thickness (taking into account the oxidation of the Al layer). Thus, we conclude that because the calculated barrier width of the Ge/C_{60} multilayers is clearly associated with the deposited thickness of the *individual* germanium layers, it appears as though the (much thicker) C_{60} layers are acting effectively as equipotential layers. This is consistent with the observed charging effects elucidated above.

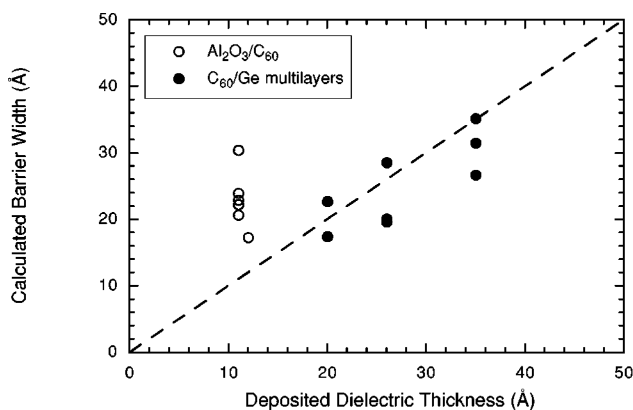

FIG. 8. Calculated barrier width as a function of the deposited barrier thickness.

TABLE II. Listed are the resistances of Ge/C_{60} multilayer junctions. A number of the junctions exhibited interesting dynamical effects, changes clearly seen in the tunneling resistance. Except where noted, the systems continued to exhibit tunneling behavior after a change. Sample numbers are from Table I.

Sample number	Initial tunneling resistance (Ω)	Resistance after first change (Ω)	Resistance after second change (Ω)
8	6		
9	201	38[a]	
10	93	78	
11	22	122	20
12	5	35	
13	240		
14	31		
15	97		

[a]No longer exhibited tunneling behavior after change.

C. Dynamical effects

Interesting dynamical effects were also observed in our multilayer Ge/C_{60} systems. In many junctions, the tunneling resistance and the size of the Coulomb blockade was observed to change drastically over the course of some measurements. In some cases the resistance would increase (e.g., sample 12 in Table II), and in others, the resistance would decrease (e.g., sample 10). Regardless of whether the resistance increased or decreased, in all of the cases but one (sample 9), the system continued to exhibit tunneling behavior after the change. For the most interesting case (sample 11), the resistance of the junction first increased and then returned to close to its initial value (see Fig. 9), continuing to exhibit tunneling behavior after each change. These changes were apparently due to physical changes in the C_{60} layers. (This dynamical behavior has also been observed in our pre-

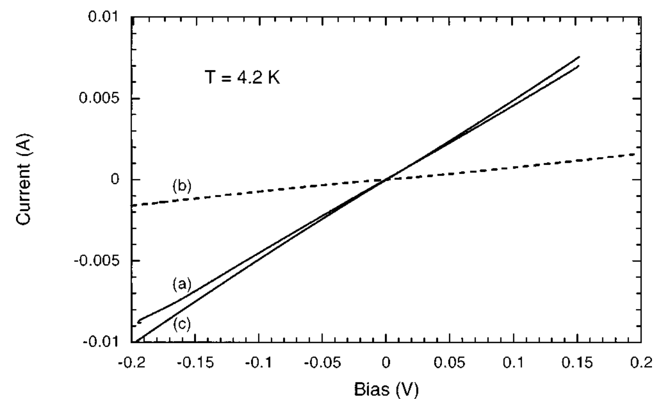

FIG. 9. An example of switching behavior in a junction where tunneling conductance significantly changes and then returns to close to its initial value. (a) The current vs voltage plot for the junction in its initial state. (b) The I-Vcurve after the junction undergoes its first change. (c) The I-Vcurve after the junction changed a second time.

liminary work on multilayer Ge/C_{70} systems.) We note that reversible changes in tunneling conductance have been reported in other disordered systems as well.[34]

IV. CONCLUSIONS

In conclusion, we have successfully prepared tunnel junctions composed of fullerene/dielectric bilayers and multilayer thin films. The thermally evaporated C_{60} and C_{70} films employed in these studies formed molecular clusters in a manner akin to the formation of droplets in thin metal films, demonstrating a systematic increase in cluster size with increasing film thickness. Our fullerene-based junctions also exhibited Coulomb blockade structure generally consistent with the size scale of the fullerene clusters and showed—at least as regards their behavior in these tunnel systems—that C_{60} clusters can act as ultrasmall capacitance systems.

Tunneling studies showed that C_{60} films less than ~400 Å thick were discontinuous. However, layered C_{60}/Ge composites showed good tunneling behavior even though the total composite thickness, ~250 Å, was in the range where both the Ge and C_{60} individually show ''pinhole''-type characteristics. Furthermore, a remarkably good correspondence between deposited Ge film thickness and calculated barrier width was found in C_{60} multilayer systems.

Finally, we note that these fullerene/dielectric tunneling systems have also exhibited interesting dynamical effects. This behavior was manifest as distinct changes—as much as an order of magnitude—in tunneling conductance. Switching behavior was also observed where junction conductance changed twice, returning to close to its original value.

ACKNOWLEDGMENTS

The authors wish to thank T. L. Peterson for the AFM work shown here and T. Kosel for STEM studies. We also wish to thank John Rowell for observations regarding the dynamical behavior of the systems. This work was supported by the Department of Energy under Grant No. DEFG02-88-ER45373.

[1] A. F. Hebard, in Phys. Today **45**(11), 26 (1992); A. F. Hebard, Annu. Rev. Mater. Sci. **23**, 159 (1993).

[2] See H. Ehrenreich and F. Spaepen, in *Solid State Physics* (Academic, San Diego, 1994), Vol. 48.

[3] A large bibliography of pre-1996 work is available at ftp physics.arizona.edu

[4] E. L. Wolf, J. Zasadzinski, J. W. Osmun, and G. B. Arnold, J. Low Temp. Phys. **40**, 19 (1980).

[5] M. Gurvitch, M. A. Washington, and H. A. Huggins, Appl. Phys. Lett. **42**, 472 (1983).

[6] E. K. Track, L.-J. Lin, G.-J. Cui, and D. E. Prober, in *Advances in Cryogenic Engineering Materials,* edited by R. P. Reed and A. F. Clark (Plenum Press, New York, 1986), pp. 635–41.

[7] S. T. Ruggiero, E. Track, D. E. Prober, G. B. Arnold, and M. J. DeWeert, Phys. Rev. B **34**, 217 (1986).

[8] J. Kwo, G. K. Wertheim, M. Gurvitch, and D. N. E. Buchanan, IEEE Trans. Magn. **19**, 795 (1983).

[9] Y. Xu, D. Ephron, and M. R. Beasley, Phys. Rev. B **52**, 2843 (1995).

[10] S. T. Ruggiero, in *Superconducting Devices,* edited by S. T. Ruggiero and D. A. Rudman (Academic, New York, 1990), pp. 373–90.

[11] M. L. A. MacVicar, J. Appl. Phys. **41**, 4765 (1970).

[12] M. L. A. MacVicar, S. M. Freake, and C. J. Adkins, J. Vac. Sci. Technol. **6**, 717 (1969).

[13] C. M. Lieber and C.-C. Chen, in *Solid State Physics* (Academic, San Diego, 1994), Vol. 48, pp. 109–48.

[14] Y. Z. Li, M. Chander, J. C. Patrin, J. H. Weaver, L. P. F. Chibante, and R. E. Smalley, Science **253**, 429 (1991).

[15] Y. Z. Li, J. C. Patrin, M. Chander, J. H. Weaver, L. P. F. Chibante, and R. E. Smalley, Science **252**, 547 (1991).

[16] G. P. Kochanski, A. F. Hebard, R. C. Haddon, and A. T. Fiory, Science **255**, 184 (1992).

[17] A. F. J. Levi and M. C. Payne, in *Proceedings of the 17th International Conference on the Physics of Semiconductors,* edited by J. D. Chadi and W. A. Harrison (Springer-Verlag, New York, 1985), pp. 913–6.

[18] J. B. Barner and S. T. Ruggiero, Phys. Rev. B **39**, 2060 (1989).

[19] E. J. van Loenen, M. Iwami, R. M. Tromp, J. F. van der Veen, and F. W. Saris, Thin Solid Films **104**, 9 (1983).

[20] S. Celaschi, J. Appl. Phys. **60**, 296 (1986).

[21] D. A. Rudman and M. R. Beasley, Appl. Phys. Lett. **36**, 1010 (1980).

[22] W. F. Brinkman, R. C. Dynes, and J. M. Rowell, J. Appl. Phys. **41**, 1915 (1970).

[23] M. Amman, R. Wilkins, E. Ben-Jacob, P. D. Maker, and R. C. Jaklevic, Phys. Rev. B **43**, 1146 (1991).

[24] A. E. Hanna and M. Tinkham, Phys. Rev. B **44**, 5919 (1991).

[25] K. Mullen, E. Ben-Jacob, R. C. Jaklevic, and Z. Schuss, Phys. Rev. B **37**, 98 (1988).

[26] J. B. Barner and S. T. Ruggiero, Phys. Rev. Lett. **59**, 807 (1987).

[27] I. Giaever and H. R. Zeller, Phys. Rev. Lett. **20**, 1504 (1968).

[28] K. K. Likharev, N. S. Bakhvalov, G. S. Kazacha, and S. I. Serdyukova, IEEE Trans. Magn. **25**, 1436 (1989).

[29] M. Amman, E. Ben-Jacob, and K. Mullen, Phys. Lett. A **142**, 431 (1989).

[30] J. G. Simmons, J. Appl. Phys. **34**, 238 (1963); J. G. Simmons, *ibid.* **34**, 1793 (1963); J. G. Simmons, *ibid.* **34**, 2581 (1963); J. G. Simmons, in *Tunneling Phenomena in Solids,* edited by E. Burstein and S. Lundquist (Plenum, New York, 1969), pp. 135–48.

[31] T. B. Ekkens, S. Nolen, and S. T. Ruggiero, J. Appl. Phys. **79**, 7392 (1996).

[32] H. Asano, K. Tanabe, O. Michikami, M. Igarashi, and M. R. Beasley, Jpn. J. Appl. Phys. **24**, 289 (1985).

[33] R. Meservey, P. M. Tedrow, and J. S. Brooks, J. Appl. Phys. **53**, 1563 (1982).

[34] S. R. Ovshinsky, Phys. Rev. Lett. **21**, 1450 (1968).